# Supporting Information for:
# 2000 Hours Photostability Testing of Dye Sensitised Solar Cells using a Cobalt Bipyridine Electrolyte

Roger Jiang,[a] Assaf Y. Andersson,[a] Piers R. F. Barnes[a] and Brian C. O'Regan*[a]

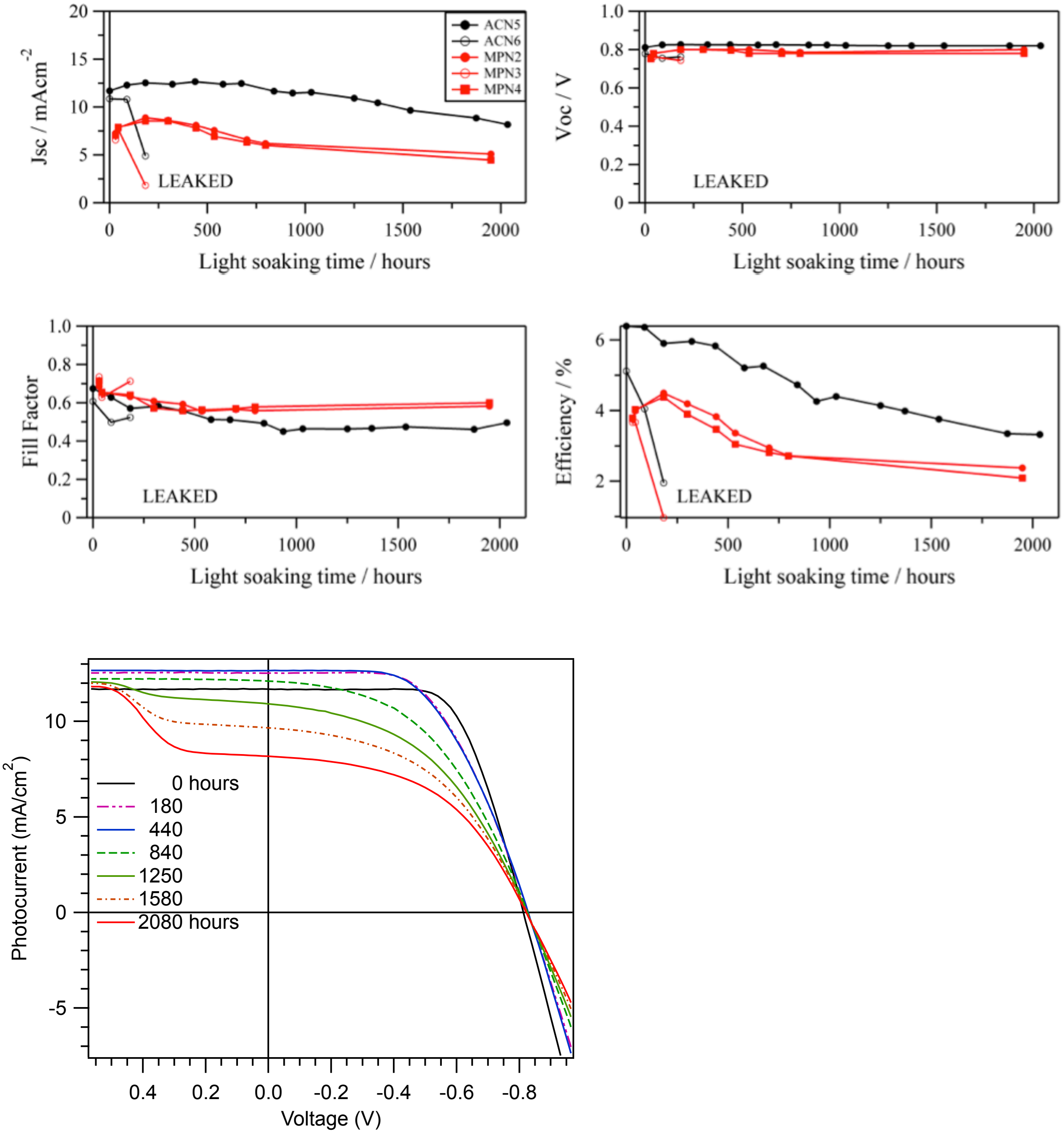

Figure S1. a-d) Additional stability data for cobalt electrolyte DSSCs under continuous LED illumination at 1 sun equivalent. Two of the cells which leaked early are shown for comparison. Evaporation may have played some part in the decay of those cells which did not visibly leak. e) Evolution of the JVs of ACN5 with illumination time. Though about 1200 hours, the evolution is similar to that of ACN2. After 1000 hours the maximum diffusion current limits the Jsc even at one sun. The application of reverse bias apparently increases the concentration or mobility of the limiting ion, leading to an (transient) increase in reverse bias photocurrent and Jsc. See the last section of this document for details.

## Recombination and Transport Measurements Concerning the Degradation of Fill Factor.

### - Electrochemical Impedance Spectroscopy

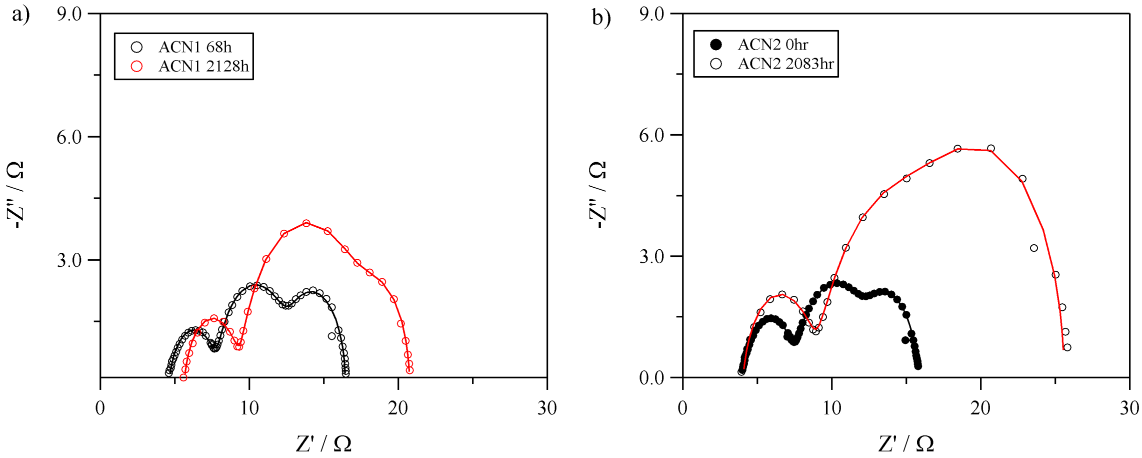

Figure S2. Nyquist plots of EIS spectra measured on ACN cells before and after light soaking for 2000 h. Experimental data (circle markers) was fitted using a standard DSSC equivalent circuit (lines).

Figure S2 shows initial and final Nyquist plots for the cells ACN1 and ACN2. Three semicircles in distinct frequency response regions are observed as expected for DSSCs. The high frequency semicircle (farthest left) corresponds to the impedance of charge transfer at the counter electrode ($R_{CE}$). The mid frequency semicircle corresponds to the impedance of recombination at the $TiO_2$/dye/electrolyte interface ($R_{PE}$). The low frequency semicircle (farthest right) corresponds to the Nernst diffusion impedance ($R_D$) in the electrolyte.

A standard equivalent circuit model was used to model the impedance spectra collected from the devices as described by the circuit diagram in figure S3.[1] As usually true with DSSCs, constant phase elements were required to fit the data. This uses two fitting parameters, $Q$ and $\beta$. When the CPE is in parallel with a resistor, $R$, the equivalent capacitance of the element can be estimated by [2]

$$C = Q^{1/\beta} R^{1/\beta - 1}.$$

Constant phase element coefficients required were between 0.8 and 0.9.

The diffusion of ions in the electrolyte is described by a Warburg impedance element (also known as Nernst Diffusion). The impedance characteristics of this element can be related to the diffusion of the minority redox species (likely to be the cobalt (III) ions) to and from the counter electrode according to the following relationship as the applied voltage is oscillated:

$$Z_d = R_D \sqrt{\frac{D}{\mathrm{i}\delta^2\omega}} \tanh\left(\sqrt{\frac{\mathrm{i}\delta^2\omega}{D}}\right)$$

$$R_D = \frac{k_B T \delta}{q^2 c D}$$

here $k_B$ is Boltzmann's constant, $T$ is the temperature, $\delta$ is the diffusion layer thickness (approximated to be the electrolyte layer thickness), $q$ is the electronic charge, $c$ is the equilibrium concentration of cobalt (III) ions, $D$ is the diffusion coefficient of these ions and $\omega$ is the angular frequency of the measurement. Thus changes in the observed Warburg impedance and the diffusion resistance $R_D$ can be related to changes in the ionic concentration of the limiting redox species if all other parameters are constant.

1. J. Halme, P. Vahermaa, K. Miettunen, and P. Lund, *Adv. Mater.*, 2010, **22**, E210–34.

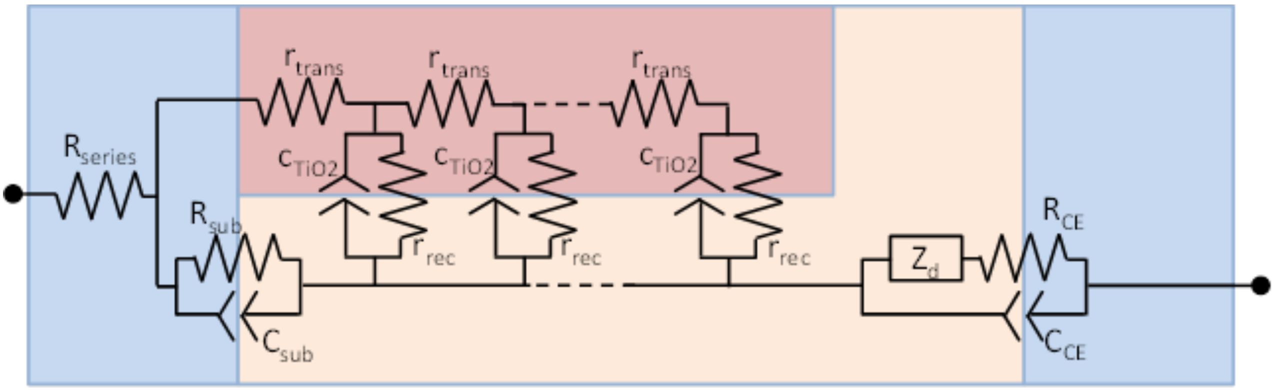

**Figure S3.** Transmission line equivalent circuit typically used to analyse the impedance spectra of DSSCs. $R_{series}$ is the series resistance of the cell, $C_{sub}$ is the capacitance of the substrate, $c_{TiO2}$ is the distributed differential capacitance of the $TiO_2$ (chemical capacitance), $r_{rec}$ is the distributed resistance to electron recombination (charge transfer) and $r_{trans}$ is the distributed resistance to electron transport. $Z_d$ is the Warburg impedance of the electrolyte, $R_{CE}$, the charge transfer resistance of the counter electrode, and $C_{CE}$ the capacitance of the counter electrode. All capacitive elements were actually modelled using constant phase elements.

Table S1. Parameters derived from the impedance analysis of the ACN cells shown in main text figures 1, 2, and 5.

| Illumination Time (hours) | Series Resistance $R_S$ | Counter Electrode $R_{CE}$ | Electrolyte Diffusion $R_D$ | $TiO_2$/Electrolyte Charge Transfer $R_{PE}$ |
|---|---|---|---|---|
| ACN2 | | | | |
| 0 | 4.01 | 3.461 | 4.051 | 4.185 |
| 88.5 | 6.17 | 4.703 | 5.48 | 4.716 |
| 183 | 6.247 | 4.664 | 5.215 | 5.198 |
| 321.5 | 6.295 | 5.052 | 5.919 | 6.15 |
| 437.5 | 4.604 | 4.718 | 6.224 | 5.733 |
| 580 | 5.224 | 4.254 | 6.907 | 5.862 |
| 673.5 | 4.024 | 5.838 | 7.161 | 6.095 |
| 840.5 | 6.252 | 6.15 | 8.379 | 6.223 |
| 935 | 4.189 | 6.132 | 8.374 | 6.566 |
| 1031 | 6.334 | 5.879 | 8.838 | 6.302 |
| 2082.5 | 4.056 | 4.677 | 10.85 | 6.007 |
| ACN1 | | | | |
| 68 | 4.596 | 3.181 | 4.796 | 3.865 |
| 132.5 | 4.765 | 3.355 | 7.244 | 4.205 |
| 227 | 6.927 | 4.498 | 9.854 | 4.507 |
| 365.5 | 6.925 | 4.557 | 8.307 | 5.541 |
| 481.5 | 5.68 | 4.228 | 7.779 | 5.224 |
| 624 | 5.224 | 4.254 | 6.907 | 5.862 |
| 717.5 | 4.898 | 4.534 | 7.162 | 5.698 |
| 884.5 | 5.002 | 4.34 | 6.846 | 6.181 |
| 979 | 4.989 | 4.308 | 6.409 | 6.588 |
| 1075 | 5.037 | 4.126 | 6.2 | 6.118 |
| 2127.5 | 5.635 | 3.635 | 4.013 | 7.47 |

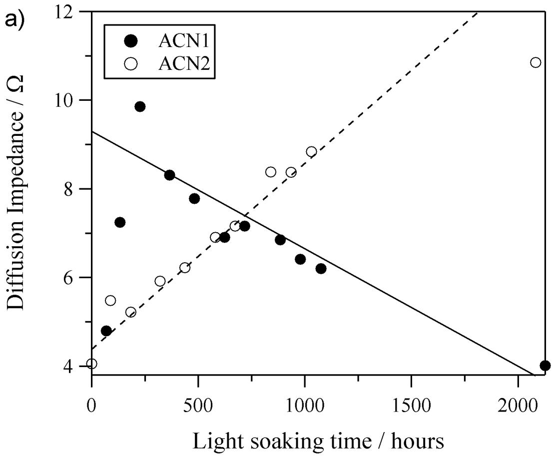

Figure S4. Evolution of the diffusion impedance with light soaking time for cell ACN1 and ACN2.

Initially, both ACN cells show almost identical Nyquist plots. Table S1 shows the gives the fit derived values for the various resistances. Figure S4 shows the changes in $R_D$ with light soaking time for the two ACN cells. Cell ACN 2 increased monotonically from 4 Ω to 10 Ω, whereas cell ACN1 increased from 5 Ω to 10 Ω and then decreased again to 4 Ω. Despite the different evolution figure there is a strong correlation between $R_D$ and the fill factor for both cells as shown figure 5 in the main text.

### - Transient and Charge Extraction Measurements

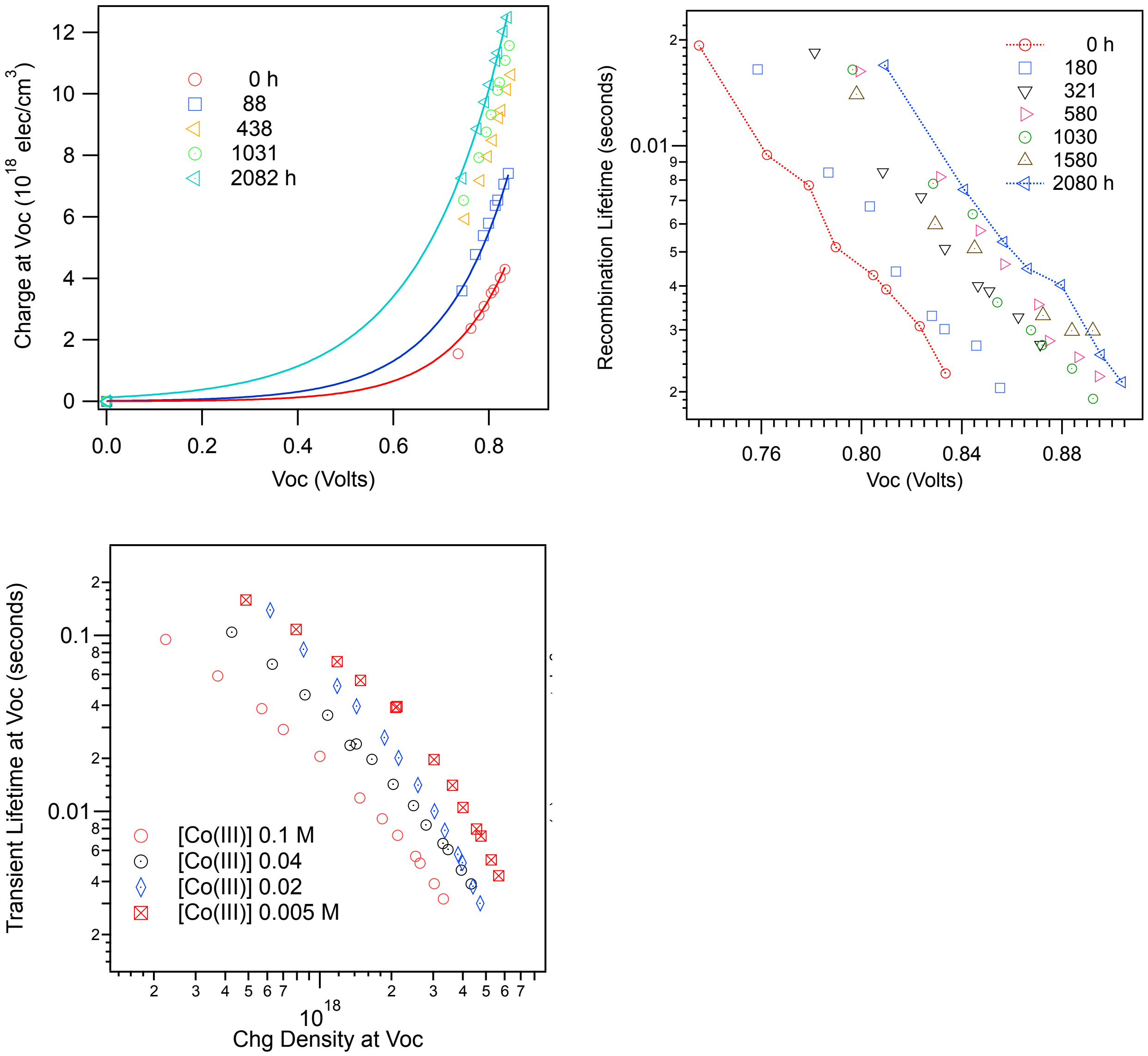

Figure S5. a) Charge density (from charge extraction) vs Voc, for cell ACN2. Charge vs Voc for other exposure times lie in sequence with that shown and have ben omitted for clarity. b) Recombination lifetime at open circuit, for cell ACN2 as measured by photovoltage transients. The lifetimes in figure S5b have been been normalized down to remove the effect of the increase in trap density with exposure time shown in figure 7a in the main text. The lifetime vs Voc points have been move to the right to correct for shifts in the conduction band edge. The shift in conduction band edge has been determined from figure S5a after normalization to take into account the increase in trap density from figure 6a, main text. c) Recombination lifetime vs charge density for cells with varying Co(III) concentrations.

In figure S5a, there is a left shift and/or up shift in the charge vs Voc data with illumination time. Some of the up shift is caused by the increase in traps indicated in figure 7a. Normalizing for a two fold increase in traps from figure 7a, figure S5a still indicates about a 60 mV downshift in the conduction band potential. In figure S5b comparison of recombination lifetimes along a vertical line should correspond to comparison of the conduction band recombination rate constant. The effects of the apparent shift in the Vcb and increase trap density have been removed in the presentation in figure S5b. It appears that there was a significant increase in lifetime up to 320 hours. From 300 hours to 2000 hours the data do not show a consistent trend, however the recombination lifetime at 2080 hours is the longest. We note without the correction for shift in

Vcb and trap density, the apparent increase in recombination lifetime would be ~5 time larger. In any case, the argument in the main text is that the degradation of the fill factor is not caused by increasing recombination. The recombination data support that argument no matter how it is normalized, and thus support the conclusion that the degradation in fill factor is caused by changes in charge transport through the electrolyte.

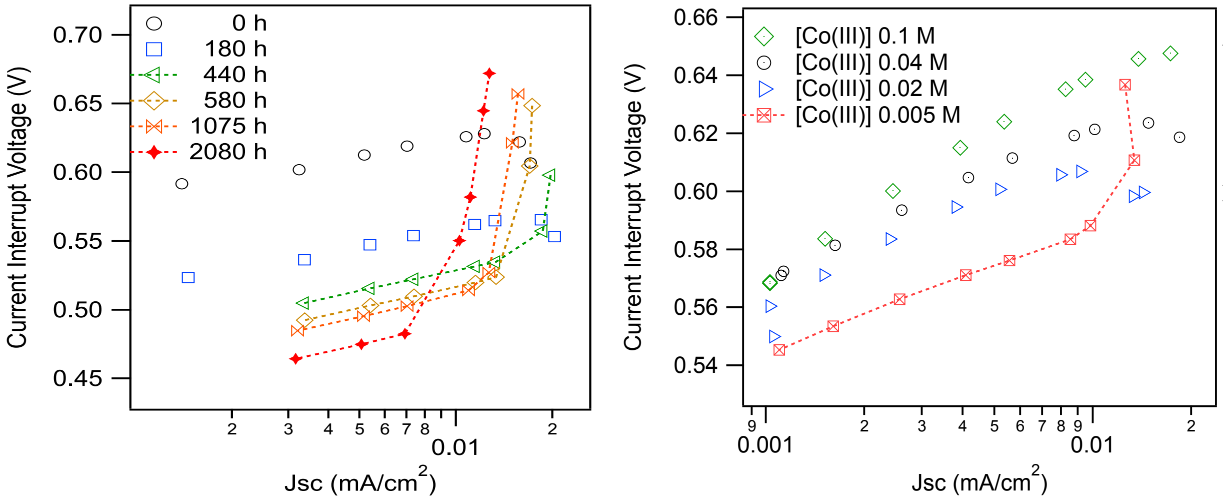

Figure S6 a) Current interrupt voltage vs Jsc for cell ACN2. b) Current interrupt voltage for cells with different Co(III) concentrations.

The current interrupt voltages in after 400 hours illumination in figure 6a resemble those of the cell with 0.005 M Co(III). Again suggesting that the illumination produces a situation of low Co(III) concentration or low ability of the Co(III) ions to escape from the TiO2 pores to reach the counter electrode. For completeness, one oddity requires mention. The current interrupt voltage decreases by about 140 mV over the illumination time. Current interrupt voltage value should not depend on trap density. This decrease is larger than the decrease in Vcb calculated above (~65 mV) To reconcile the two might require that the Li+ induced traps actually lower the energy of the "transport level" (mobility edge) below that of the "recombination level."

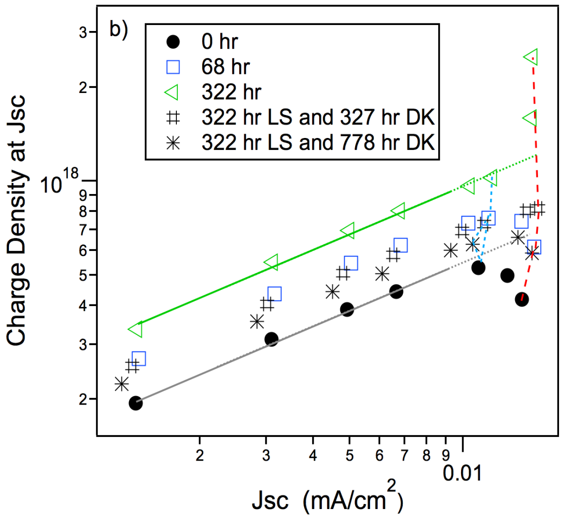

Figure S7 Evolution of charge and SC in cell ACN3 was light soaked for 322 hours then held 778 hours in the dark and ~20 °C (markers * and #). One sun points are connected by the blue dotted line. Two sun points are connected by the red dashed line.

## Charge extraction from short-circuit measurements made on iodine-based DSSCs

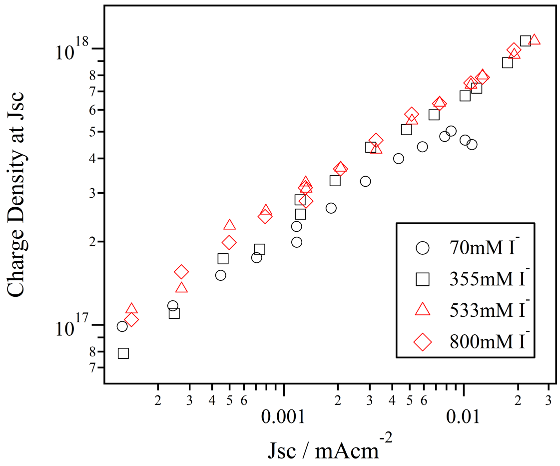

Figure S8. Charge density in $TiO_2$ vs. the $J_{sc}$. Charge was measured by charge extraction from short circuit. $J_{sc}$ was varied using a range of light intensities from ~0.007 Sun to ~2.4 Sun. 4 different cells containing iodine/ iodide electrolyte was tested. Keeping all other parameters constant, the electrolyte was varied with respect to iodide concentration. Electrolyte composition: X M 1-propyl-3-methyl imidazolium iodide (PMMI) (where X = 70, 355, 533 and 800 mM), 0.3 M benzimidazole, 0.05 M guanidinum thiocyanate and 0.05 M iodine in 3-methoxypropionitrile (MPN). 1-Propyl-3-methyl imidazolium-bis(trifluoromethylsulfo- nyl)imide (PMMTFSI) was substituted for the iodide salt to keep the PMM+ concentration constant.Further details of the cells are discussed elsewhere.[2]

2. A. Y. Anderson, P. R. F. Barnes, J. R. Durrant, and B. C. O'Regan, *J. Phys. Chem. C*, 2011, **115**, 2439–2447.

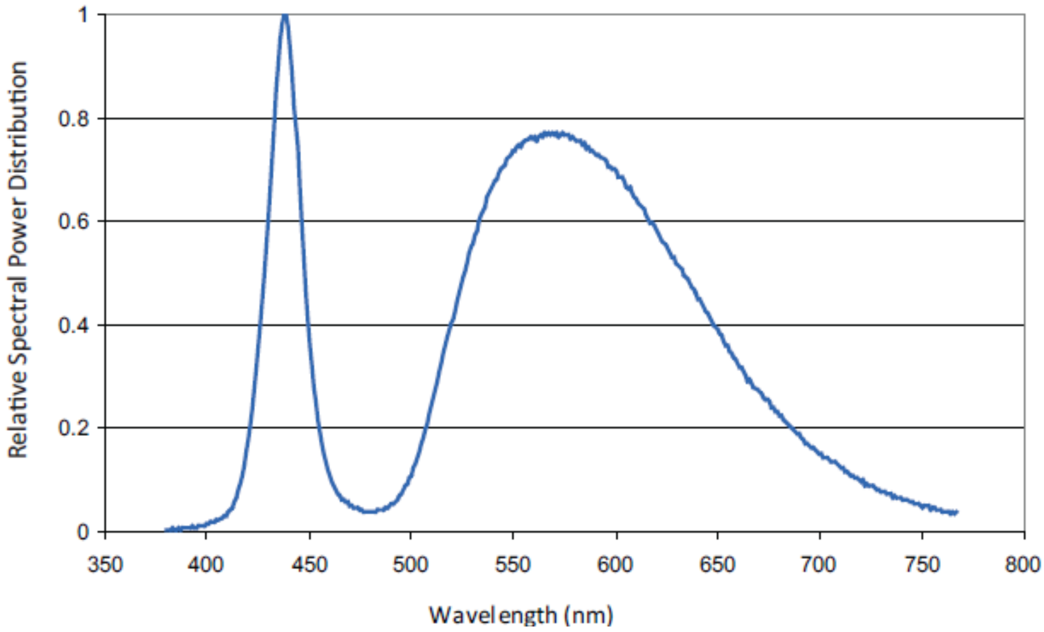

FIgure S9. Typical output spectrum of white LEDs with colour temperature 4000 K, as used in the LED array for the illumination in this article. The specific LEDs used were Osram LCW W5AM-KXKZ-4L8N.

## Hysteresis in the *J-V*s for some degraded cells

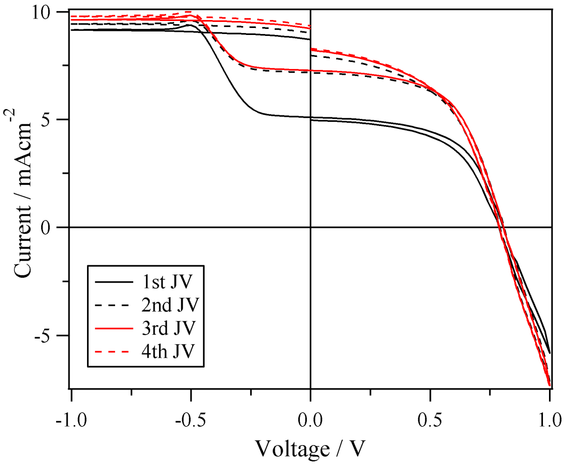

Figure S10. 1 Sun *J-V* characteristics of a cobalt DSSC containing MPN electrolyte (MPN2). This was measured after the cell had leaked electrolyte. A total of 4 *J-Vs* were measured for the same cell. Each *J-V* was measured cyclically starting from 0 V going to +1 V, then -1 V and back to 0 V. Each consecutive *J-V* was measured directly after the previous *J-V* measurement.

During the 2000 h light soaking test, there was a heating incident (see experimental section). The heating resulted in some cells leaking electrolyte. The following discussion applies to the cells which degraded due to electrolyte leakage. It does not apply to the cells discussed in the paper (ACN1, ACN2, ACN3, ACN4 and MPN1). The following discussion will be relevant to all the cells which we discarded in this experiment (ACN5, ACN6, MPN2, MPN3 and MPN4). It is worth noting that all the discarded cells shared similar characteristic hysteresis in the *J-V* curves (Figure S10). We do not know for certain if this effect occurs exclusively due to partial electrolyte leakage.

Figure S10 shows consecutive cyclic *J-V* measurements made on the same cell (MPN2). Each *J-V* set was measured cyclically starting from 0 V going to +1 V, then -1 V and back to 0 V. The initial $J_{sc}$ was ~5 mAcm$^{-2}$. After scanning in reverse bias direction the photocurrent increased. Upon returning to 0V, the final $J_{sc}$ was ~8.5 mAcm$^{-2}$. When a second *J-V* was directly measured after this, the initial $J_{sc}$ was ~8 mAcm$^{-2}$ and the final $J_{sc}$ was ~9 mAcm$^{-2}$. With repeated the cyclic *J-V* measurements, the apparent performance improved due to higher $J_{sc}$. However, this increase in $J_{sc}$ was temporary. Within hours, the $J_{sc}$ decreased back to the initial value (~5 mAcm$^{-2}$). We have also observed that this effect only occurs when this cell was exposed to light and put in reverse bias. When the cell was scanned in reverse bias in the dark, there was no such improvement in the $J_{sc}$ (in subsequent 1 Sun *J-V* measurements). We do not as of yet have a proposed mechanism for this effect. The photocurrent increase in reverse bias and under light could correspond to a transient increase in the number of Co(III) species. The required condition for this hysteresis effect to occur (which are illumination and reverse bias) suggests a possible photochemical reaction process is occurring.

It is important to note that such hysteresis effects could potentially lead to misleading interpretation of cell stability. In order to identify these hysteresis effects we have proposed a number of procedures in our JV measurements. Firstly, we report only the first set of *J-V* measurements in our paper. Therefore, a hysteresis such as in Figure S10 can be immediately identified. Secondly, all the JV measurements were initiated at 0 V and scanned cyclically (as already discussed). Lastly, we monitored the $J_{sc}$ stability up to 10 seconds prior to each *J-V*. and compared it to the final graph. We only continued measuring cells which produce *J-V*s with almost no hysteresis and stable $J_{sc}$. The cells which early on showed hysteresis or unstable $J_{sc}$ such as in Figure S10 were discarded from the experiment, However, ACN5 was carried though, as shown in figure S1c.